Available online at www.sciencedirect.com
ScienceDirect
International Journal of Multiphase Flow 33 (2007) 970–986
International Journal of Multiphase Flow
www.elsevier.com/locate/ijmulflow

Interaction between Taylor bubbles rising in stagnant non-Newtonian fluids

R.G. Sousa, A.M.F.R. Pinto, J.B.L.M. Campos *

Centro de Estudos de Fenómenos de Transporte, Departamento de Engenharia Química, Faculdade de Engenharia da Universidade do Porto, Rua Dr. Roberto Frias 4200-465 Porto, Portugal

Received 9 March 2006; received in revised form 28 March 2007

Abstract

The interaction between Taylor bubbles rising in stagnant non-Newtonian solutions was studied. Aqueous solutions of carboxymethylcellulose (CMC) and polyacrylamide (PAA) polymers were used to study the effect of different rheological properties: shear viscosity and viscoelasticity. The solutions studied covered a range of Reynolds numbers between 10 and 714, and Deborah numbers up to 14. The study was performed with pairs of Taylor bubbles rising in a vertical column (0.032 m internal diameter) filled with stagnant liquid. The velocities of the leading and trailing bubbles were measured by sets of laser diodes/photocells placed along the column. The velocity of the trailing bubble was analysed together with the liquid velocity profile in the wake of a single rising bubble (Particle Image Velocimetry data obtained from the literature). For the less concentrated CMC solutions, with moderate shear viscosity and low viscoelasticity, the interaction between Taylor bubbles was similar to that found in Newtonian fluids. For the most concentrated CMC solution, which has high shear viscosity and moderate viscoelasticity, a negative wake forms behind the Taylor bubbles, inhibiting coalescence since the bubbles maintain a minimum distance of about 1D between them. For the PAA solutions, with moderate shear viscosity but higher viscoelasticity than the CMC solutions, longer wake lengths are seen, which are responsible for trailing bubble acceleration at greater distances from the leading bubble. Also in the PAA solutions, the long time needed for the fluid to recover its initial shear viscosity after the passage of the first bubble makes the fluid less resistant to the trailing bubble flow. Hence, the trailing bubble can travel at a higher velocity than the leading bubble, even at distances above 90D.

Keywords: Taylor bubble; Coalescence; Non-Newtonian fluids; Viscoelasticity

1. Introduction

Slug flow is a two-phase flow regime found when a gas and a liquid flow simultaneously in a pipe over certain flow rate ranges. It is characterised by elongated gas bubbles (Taylor bubbles or slugs) which almost

* Corresponding author. Fax: +351 225081449.
E-mail address: jmc@fe.up.pt (J.B.L.M. Campos).

0301-9322/$ - see front matter © 2007 Elsevier Ltd. All rights reserved.
doi:10.1016/j.ijmultiphaseflow.2007.03.009

fill the pipe cross-section, and the liquid flows around and between the bubbles. The liquid flowing around the bubble forms a falling film which separates from the end of the bubble, creating a liquid wake attached to the bubble and travelling at the same upward mean velocity. The flow pattern in the wake can be laminar or turbulent (Campos and Guedes de Carvalho, 1988). This type of slug flow regime is found in a number of industrial processes, such as geothermal systems, oil and gas wells, fermentation, among others. In some chemical processes slug flow is used to increase the reaction rate due to the efficient mixing of reagents in the turbulent wake of Taylor bubbles.

The velocity of the bubble depends on the velocity of the liquid ahead of it (Moissis and Griffith, 1962), among other physical and geometrical parameters. When two or more bubbles rise simultaneously in a column the wake of the leading bubble can affect the velocity of the trailing one, and usually induces coalescence of bubbles. This mechanism has been studied by several authors. Shemer and Barnea (1987) explained the interaction between bubbles flowing in water by relating the velocity of the trailing bubble to the maximum instantaneous liquid velocity ahead of its nose. Three regions were observed:

- In the near wake region of the leading bubble ($z^*/D < 2$, where z^* is the distance to the bubble trailing edge and D the column internal diameter, Fig. 1), the velocity profile is highly distorted by the tumbling of the falling film. A steep decrease of the maximum instantaneous liquid velocity in each cross-section is observed as the distance to the bubble trailing edge increases.
- For $z^*/D > 2$, a much more gradual decrease of the maximum instantaneous liquid velocity is observed, despite the strong radial flow oscillations. When the nose of the trailing bubble is inside this region it moves radially, trying to follow the random radial movement of the maximum liquid velocity ahead.
- At $z^*/D > 12$ the velocity profile, although still distorted, does not differ much from a fully developed one.

Pinto and Campos (1996) conducted studies on the coalescence of pairs of Taylor bubbles (see Fig. 1) rising in stagnant vertical Newtonian liquid columns, covering a wide range of liquid viscosities in three column diameters. These authors applied a technique based on the signals of differential pressure transducers, to determine the distance between bubbles above which there is no interaction, l_{min}, and also to establish the approach

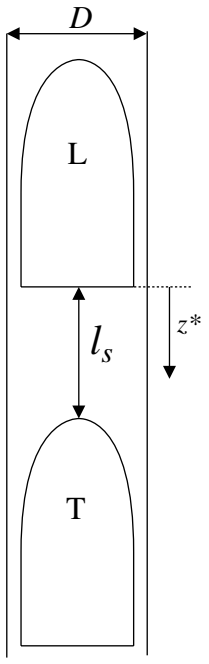

Fig. 1. Diagram representing the leading (L) and trailing (T) Taylor bubbles, the distance between them, l_s, and distance to the bubble trailing edge, z^*.

velocity of the trailing bubble as a function of the distance between bubbles, l_s. Correlations were found between l_{min} and a modified Reynolds number defined as $N_f = D^{3/2}g^{1/2}\rho/\mu$ (Pinto and Campos, 1996), where g is the gravity acceleration, ρ and μ the liquid density and viscosity, respectively. The correlations were established for different wake regimes:

Laminar

$$\frac{l_{min}}{D} = 1.46 + 4.75 \times 10^{-3} N_f, \quad 100 < N_f < 500 \tag{1}$$

Transition

$$\frac{l_{min}}{D} = 6.92 \times 10^{-1} + 7.90 \times 10^{-3} N_f, \quad 500 < N_f < 1500 \tag{2}$$

Turbulent

$$\frac{l_{min}}{D} = 12.5, \quad N_f > 1500 \tag{3}$$

The authors compared l_{min} with the wake lengths, l_w, determined by Campos and Guedes de Carvalho (1988), and found a constant ratio between them ($l_w/l_{min} = 0.24$, independent of the wake regime). The ratio between the velocities of the trailing (U_T) and leading (U_L) bubbles is related to the normalised distance between bubbles by

$$\frac{U_T}{U_L} = -11.4\frac{l_s}{l_{min}} + 4.24, \quad l_s/l_{min} < 0.24 \tag{4}$$

$$\frac{U_T}{U_L} = 2.01 - 1.96\frac{l_s}{l_{min}} + 0.95\left(\frac{l_s}{l_{min}}\right)^2, \quad l_s/l_{min} > 0.24 \tag{5}$$

Similar studies on coalescence of pairs of Taylor bubbles rising in co-current flowing Newtonian liquid were conducted by Pinto et al. (1998, 2001a, 2005).

Talvy et al. (2000) studied the interaction between two consecutive Taylor bubbles rising in stagnant water, using an image processing technique. An effective acceleration of the trailing bubble in the near wake region was observed, despite some instantaneous decelerations. Even at distances exceeding 50 column diameters from the leading bubble trailing edge, an influence on the trailing bubble velocity was observed (turbulent wake conditions).

All of this previous research was with Newtonian fluids. However, there are many industrial processes where the liquid is non-Newtonian, such as in biological and waste-treatment air-lift reactors and polymer devolatilisation processes. It is well known that some features of non-Newtonian liquids, mainly their viscoelasticity, are responsible for strange phenomena such as the climbing rod, the tubeless siphon and the Ueber effect. Research on slug flow in non-Newtonian fluids remains scarce. Sousa et al. (2004, 2005) used PIV technique to study the flow around individual Taylor bubbles rising in aqueous solutions of carboxymethylcellulose (CMC), with different weight percentages of Polymer (a shear-thinning fluid with low viscoelasticity). The authors describe the wake flow patterns behind the Taylor bubbles for a range of Reynolds numbers between 4 and 714, and Deborah numbers up to 0.236. From the highest to the lowest values of Reynolds number the wake flow pattern changes, from a three dimensional oscillating flow to a negative (opposite direction to the bubble displacement) wake flow. In the middle range, axi-symmetric closed wakes were found. Later, (Sousa et al., 2006) performed similar studies with aqueous solutions of polyacrylamide (PAA), a polymer with a higher viscoelasticity. The study covered a range of Reynolds numbers between 2 and 1158, and Deborah numbers up to 115. The wake flow patterns differ from those found in CMC solutions. Even for the lower Deborah numbers a central (near the axis) region with the fluid being stretched was found.

There is little information in the literature about coalescence of Taylor bubbles in non-Newtonian fluids. There are some studies about the coalescence of small bubbles in non-Newtonian fluids (Kee et al., 1990; Li et al., 1997a,b, 1998, 2001) where the viscoelastic effects are described. In the present work a study on the interaction between consecutive Taylor bubbles rising in the CMC and PAA solutions used by Sousa

et al. (2005, 2006) is reported. The liquid flow patterns obtained in the previous PIV studies are linked with the approach velocity of the trailing bubble to the leading one.

2. Experiments

The experimental study was performed by injecting pairs of Taylor bubbles into a vertical tube at different instants and analyzing any interaction during their rise. It was done in a vertical acrylic column having a height of 7 m and a 32 mm internal diameter.

Two lateral tubes connected to the main column at the bottom, as shown in Fig. 2, worked as the bubble injection system. In each injection tube, two globe valves (V_A and V_B) facilitated the launch of a Taylor bubble; opening the upper valve released the air trapped between the valves into the main column. The studies were made with the top of the column closed, to avoid any effect of gas expansion on the bubble velocity (valve V_D).

Six sets of laser diodes/photocells were used in the experiments. Each laser diode emits light through the column, aimed at a photocell. When a bubble passes in front of the laser, the photocell signal drops abruptly. The bubble velocity, bubble length (L_B) and distance between bubbles are determined from the known distance between photocells, Δh, and the time lag between their signals, as shown in Fig. 3.

The laser diodes/photocells were placed in pairs along the column in order to study long distance interaction between bubbles or, in an alternative configuration, all sets were placed close together to study bubble interaction just before coalescence (see Fig. 2).

3. Rheological data

In this work, six different solutions were used: four aqueous solutions of carboxymethylcellulose (molecular weight of 3×10^5 kg kmol^{-1}, grade 7H4C from Hercules) and two aqueous solutions of polyacrylamide (Separan AP30, molecular weight of 2×10^7 kg kmol^{-1}). The solutions studied in this work were chosen from those used by Sousa et al. (2005, 2006) in PIV flow pattern studies.

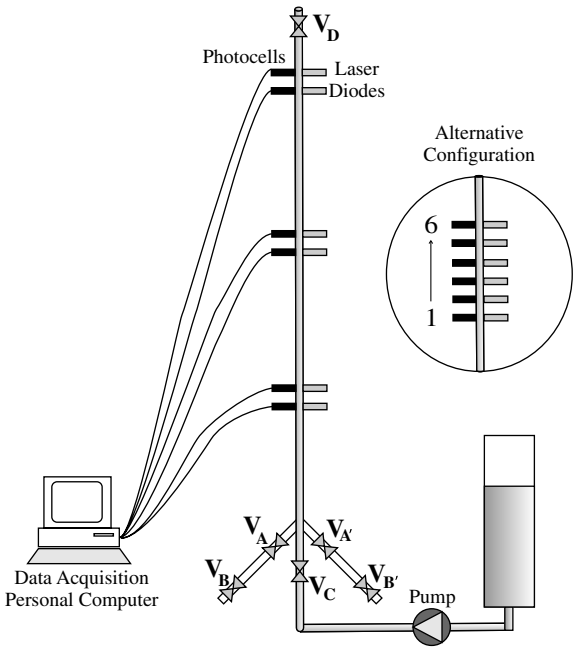

Fig. 2. Experimental setup used in the bubble interaction studies.

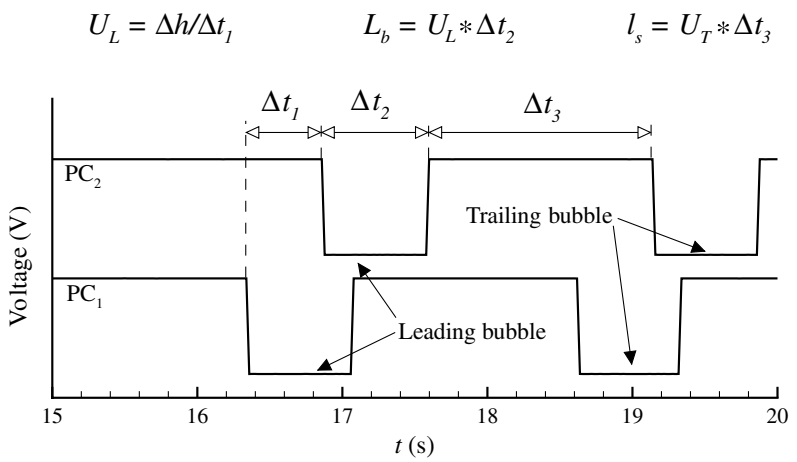

Fig. 3. Signals from two photocells when a pair of bubbles rises up the column, and the methodology used to determine bubble velocity, length and distance between bubbles.

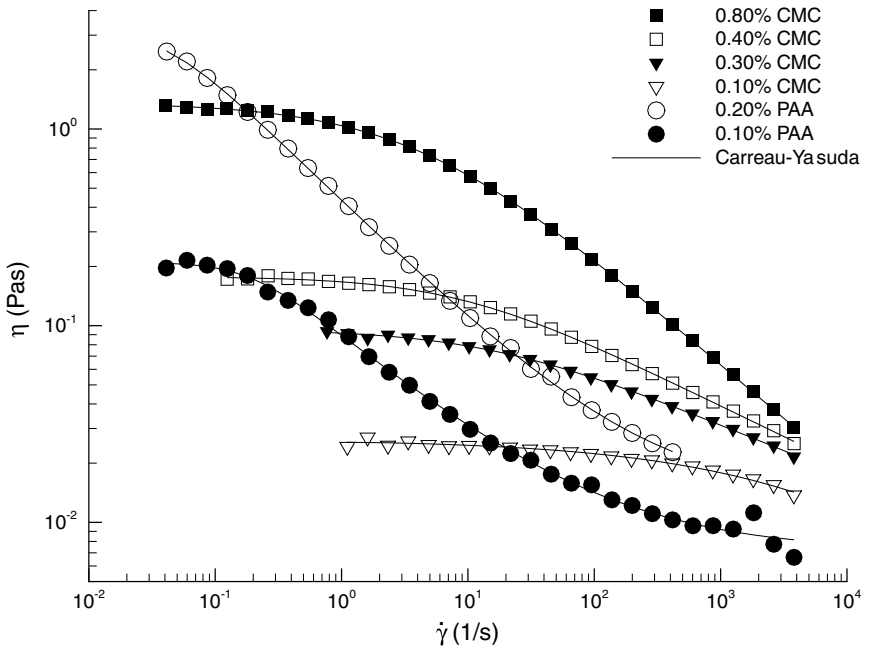

Fig. 4. Representation of shear viscosity as a function of shear rate for the solutions studied.

The shear viscosity of the solutions, η, is represented in Fig. 4 as a function of shear rate, $\dot{\gamma}$. This figure shows a steeper variation of shear viscosity for the PAA solutions. At low shear rates and for the same weight percentage of polymer, the shear viscosity of the PAA solutions is higher than that of the CMC solutions. The Carreau–Yasuda viscosity model:

$$\eta(\dot{\gamma}) = \eta_\infty + (\eta_0 - \eta_\infty)(1 + (\lambda\dot{\gamma})^{a_1})^{\frac{a_2-1}{a_1}} \tag{6}$$

was fitted to the experimental data and is represented in Fig. 4 by the solid lines. The parameters of the Carreau–Yasuda viscosity model are presented in Table 1, where T is the experimental temperature, η_0 the viscosity limit at zero shear rate, η_∞ the viscosity limit at infinite shear rate, λ a time constant, a_1 and a_2 dimensionless parameters.

Table 1
Parameters of the Carreau–Yasuda viscosity model for the studied solutions

Solution	T (°C)	η_0 (Pa s)	η_∞ (Pa s)	λ (s)	a_1	a_2	$\dot{\gamma}$ (s^{-1})
0.10 wt% CMC	20.3	0.009	0.001	0.021	0.850	0.871	1–4000
0.30 wt% CMC	21.5	0.051	0.001	0.057	0.712	0.721	0.7–4000
0.40 wt% CMC	19.0	0.110	0.001	0.110	0.809	0.675	0.125–4000
0.80 wt% CMC	22.0	1.050	0.001	0.221	0.661	0.433	0.04–4000
0.10 wt% PAA	19.8	0.210	0.007	5.321	2.007	0.464	0.04–500
0.20 wt% PAA	20.9	3.201	0.013	24.99	1.795	0.372	0.04–4200

The first normal stress difference, N_1, is represented in Fig. 5 for the PAA solutions and for the most concentrated CMC solution. For diluted CMC solutions the first normal stress difference is below the sensitivity of the rheometer. From this figure it is clear that for high shear rates the PAA solutions have a higher first normal stress difference than the CMC solution, which is four times more concentrated.

The Deborah number was defined as $De = \tau \cdot \dot{\gamma}_f$ and the Reynolds number as $Re = \rho U_b D/\eta_f$, where τ is the relaxation time of the fluids, U_{rmb} the velocity of an isolated bubble, $\dot{\gamma}_f = U_b/D$ is the characteristic shear rate of the flow and η_f the shear viscosity of the liquid at that shear rate.

The fluid relaxation time, τ, was estimated using the method of Leider and Bird (1974). Assuming that both N_1 and the shear stress, σ_{yx}, can be well approximated by power functions of the shear rate over the range of conditions of interest, i.e., $N_1 = m_1(\dot{\gamma})^{s_1}$ and $\sigma_{yx} = m_2(\dot{\gamma})^{s_2}$, the fluid relaxation time can be given by

$$\tau = \left(\frac{m_1}{2m_2}\right)^{\frac{1}{s_1 - s_2}} \tag{7}$$

The Reynolds and Deborah numbers were determined for the studied solutions and are presented in Table 2 with the bubble velocity and the relaxation time of the solutions. Although the Deborah number could not be determined for all the solutions, it is perceptible, from this table and from Sousa et al. (2005, 2006), that the PAA solutions and the most concentrated CMC solution have a more accentuated elastic behaviour.

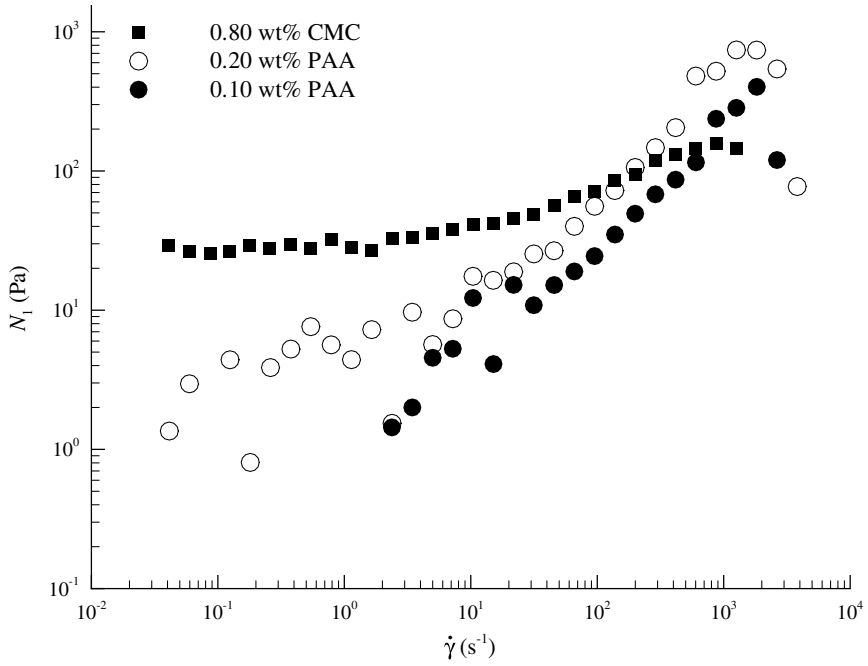

Fig. 5. Representation of the first normal stress difference as a function of shear rate for the 0.10 wt% and 0.20 wt% PAA solutions and 0.80 wt% CMC solution.

Table 2
Values of the velocity of an isolated bubble, relaxation time, Reynolds number and Deborah number

Solution	U_b	τ (s)	Re	De
0.80 wt% CMC	0.180	0.03	10	0.2
0.40 wt% CMC	0.195	–	70	≈0
0.30 wt% CMC	0.198	–	144	≈0
0.10 wt% CMC	0.199	–	714	≈0
0.20 wt% PAA	0.196	2.30	41	14
0.10 wt% PAA	0.198	$<10^{-9}$	162	≈0

4. Results

The liquid ahead of the nose of an isolated bubble is, for all the solutions, disturbed by bubble rise only in a very short distance. According to Sousa (2005), this distance is about $0.7D$, while in the range $0.3D$ to $0.7D$ the flow is slightly disturbed. Therefore, the profile ahead of the nose of a trailing bubble can be taken as similar to the one in the wake of an isolated bubble, i.e., the effect of the bubble rise can be neglected. The velocity of the trailing bubble will then be analysed together with the liquid profile in the wake of an isolated rising bubble.

4.1. CMC solutions

The 0.10 wt% CMC solution has the highest value of Reynolds number. In Sousa et al. (2005) using PIV technique, the flow around the Taylor bubbles rising in this solution showed a very unstable wake, with 3D oscillations of the bubble trailing edge. Inside the wake, some vortices were seen in continuous displacement and the upward liquid velocity was up to four times higher than the bubble velocity. Following the wake a train of small bubbles was frequently observed extending over several diameters, which did not allow for quick stagnation of the liquid after the passage of the bubble. In Fig. 6 the average flow field in the wake of Taylor bubbles rising in a 0.10 wt% CMC solution is represented (r is the radial distance to the column axis) along with the streamlines in a reference frame moving with the bubble. The average flow fields presented in this work were determined from 20 instantaneous velocity fields. Despite all the oscillations present in the wakes of Taylor bubbles rising in 0.10 wt% CMC solutions, Sousa et al. (2005), the average flow field shows a structure similar to those found in more concentrated solutions. The liquid film separates from the bubble at the trailing edge and surrounds an upward moving liquid region behind the bubble.

In the interaction studies, pairs of Taylor bubbles with different time lags between them were injected into a CMC solution. The ratio between the trailing bubble velocity, U_T and the leading bubble velocity U_L is represented in Fig. 7 as a function of the distance between bubbles, l_s.

This figure shows that below $l_s = 10D$, the ratio between the velocity of the bubbles increases as the distance between bubbles decreases, indicating an acceleration of the trailing bubble as it approaches the leading one. This ratio increases up to 5 when the distance is about $1D$. For $l_s > 10D$, the ratio between bubbles velocity tends to 1, although at some instants the trailing bubble still travels faster than the leading one, due to the disturbance caused by the small bubbles.

In Fig. 8, the trailing bubble velocity is represented as a function of the distance between bubbles along with an instantaneous vertical liquid velocity profile at the axis of the column behind an isolated Taylor bubble (obtained from Sousa et al. (2005)). An average of 20 instantaneous liquid velocity profiles ($V_{z(r=0)}$) is also plotted. Despite the radial oscillations present in the wake flow pattern, Fig. 8 shows the influence of the flow pattern in the wake of the leading bubble on the velocity of the trailing one. For $l_s > 4D$, the liquid velocity in the wake of a bubble is only perturbed by the passage of small gas bubbles that rise behind the Taylor bubble. This causes some oscillations on the liquid velocity, but do not influence significantly the trailing Taylor bubble velocity. For $1D < l_s < 4D$, the liquid velocity is moving downwards in the centre of the column, after reattachment of the liquid film. Although liquid is moving downwards in the centre, it is moving upwards in higher radial positions of the column (Fig. 6). The trailing bubble nose oscillates searching for the less resistant path in liquid with higher upward velocity, and this leads to an increased velocity for this bubble. In the region

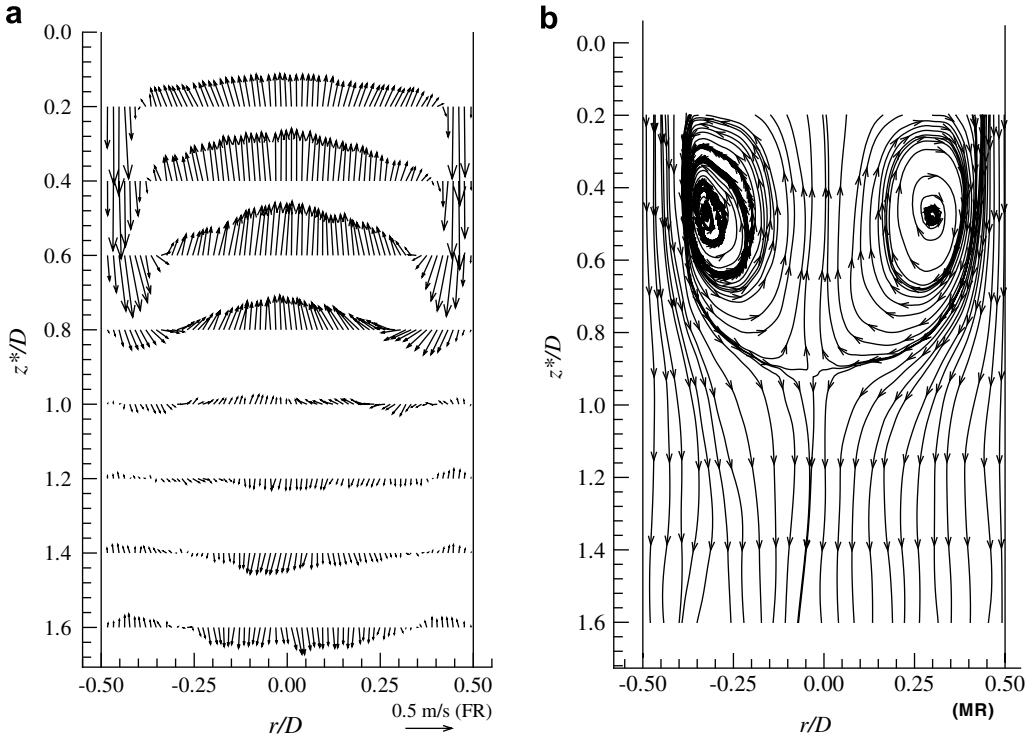

Fig. 6. (a) Average flow field (fixed reference fame) and (b) streamlines (reference frame moving with the bubble), in the wake of Taylor bubbles rising in 0.10 wt% CMC solutions.

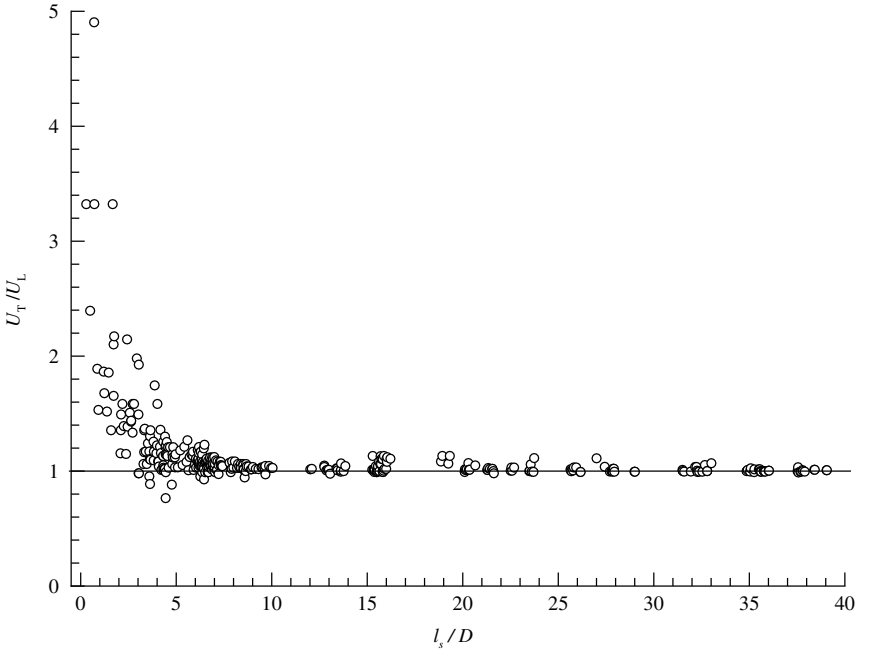

Fig. 7. Representation of the ratio between the trailing and leading bubble velocities, U_T/U_L, as a function of the distance between bubbles, l_s, for the 0.10 wt% CMC solution.

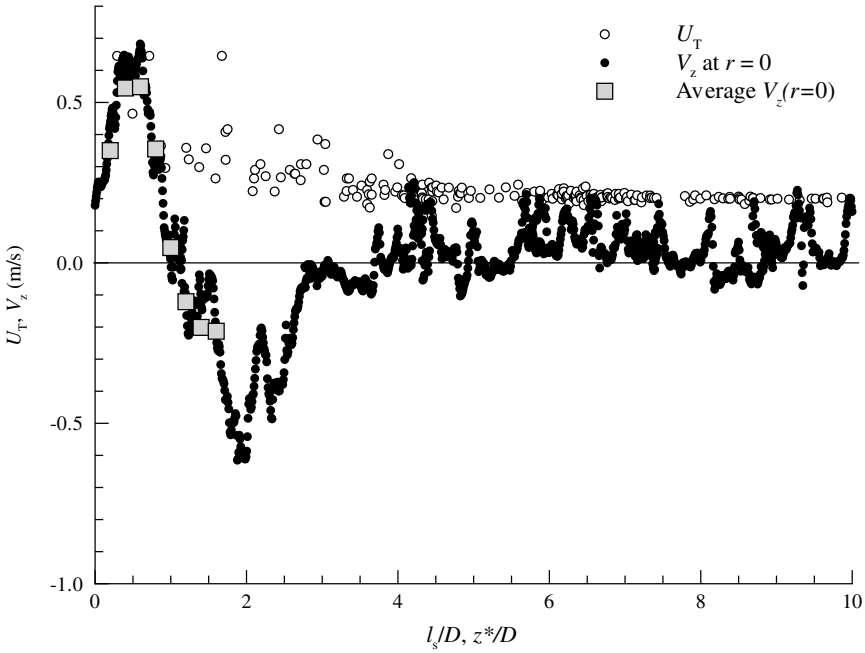

Fig. 8. Representation of the trailing bubble velocities, U_T, as a function of the distance between bubbles, l_s, and the instantaneous and average liquid vertical velocity, $V_{z(r=0)}$, as a function of the distance to the trailing edge of the leading bubble, z^*, for a 0.10 wt% CMC solution.

closer to the leading bubble trailing edge, $l_s < 1D$, the trailing bubble velocity increase is steeper, due to the upward moving liquid in the centre of the column after the passage of the leading bubble (Fig. 6).

The 0.30 wt% and 0.40 wt% CMC solutions presented a similar wake flow pattern, with a closed recirculation region. The average flow fields in the wake of Taylor bubbles rising in a 0.30 wt% CMC solution (a) and 0.40 wt% CMC solution (b) are presented in Fig. 9, with the respective streamlines in a reference frame moving with the bubble, where a longer wake length is observed for the 0.30 wt% CMC solution.

The instantaneous and average vertical liquid velocity at the axis of the column are represented in Fig. 10 as a function of the distance to the trailing edge of the Taylor bubble for both solutions.

The ratio between the trailing bubble velocity and the leading bubble velocity is represented in Fig. 11 for the 0.30 wt% and 0.40 wt% CMC solutions. This figure shows very similar behaviour for both solutions, although in the 0.30 wt% CMC solution the velocity increase in the trailing bubble occurs at a slightly greater distance from the leading bubble than in the 0.40 wt% CMC solution, due to the longer wake length, as can be also confirmed in Fig. 10. The solutions described until here had moderate shear viscosity and low (unmeasurable) viscoelasticity, showing a behaviour similar to that found in Newtonian fluids.

In the 0.80 wt% CMC solution, where besides a higher viscosity, it was already measured some viscoelasticity, the PIV studies from Sousa et al. (2005) showed a negative wake behind rising Taylor bubbles. This means that in the axis of the column the liquid is moving downwards immediately after the bubble trailing edge, in contrast to the cases previously analysed. In Fig. 12, the average flow field in the wake of a Taylor bubble rising in a 0.80 wt% CMC solution is represented (fixed reference frame), along with the streamlines in a reference frame moving with the bubble.

Initially, there were some uncertainties about the behaviour of the trailing bubble. Would the downward-moving liquid allow capture of the leading bubble by the trailing one or not? Would the trailing bubble nose deviate from this downward flow and still coalesce with the leading bubble or not? As the present work shows, for the first time, the presence of a negative wake behind a Taylor bubble is an inhibitor of coalescence. As shown in Fig. 13, the trailing bubble does not accelerate when approaching the leading bubble and maintains a minimum distance of about $1D$ due to the downward liquid movement in the wake of the leading bubble.

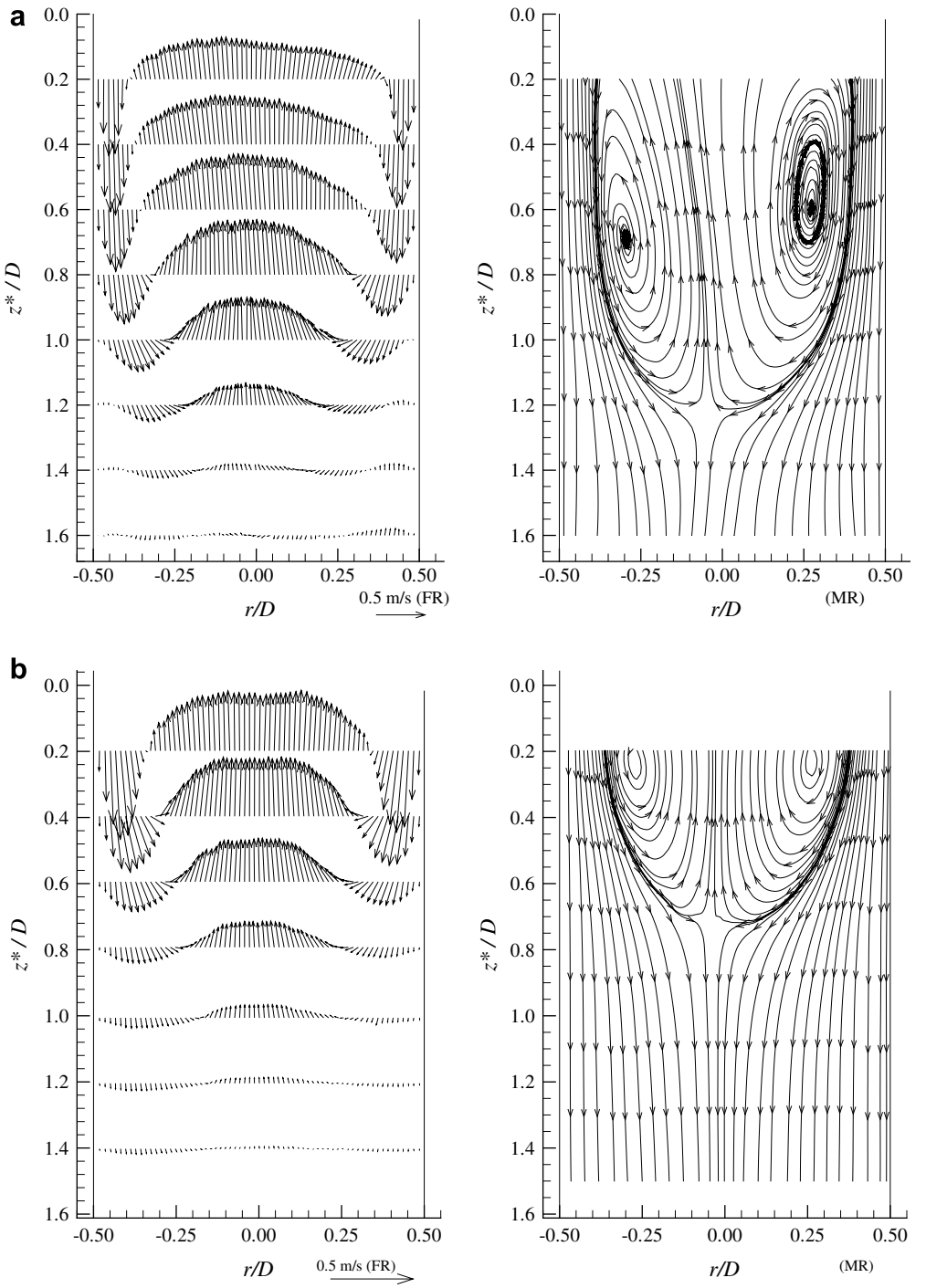

Fig. 9. Average flow fields (fixed reference frame) and streamlines (reference frame moving with the bubble), in the wake of Taylor bubbles rising in (a) 0.30 wt% and (b) 0.40 wt% CMC solutions.

The behaviour found in the 0.80 wt% CMC solution is very different from that found in Newtonian solutions, where no negative wakes are formed. Nogueira (2005) reported that the rear of a Taylor bubble rising in a stagnant column of glycerol ($Re = 3$) has a concave shape, quite different from the lacrimal shape found in the negative wake of the 0.80 wt% CMC solution. In the glycerol solution, very close to the bubble rear, there

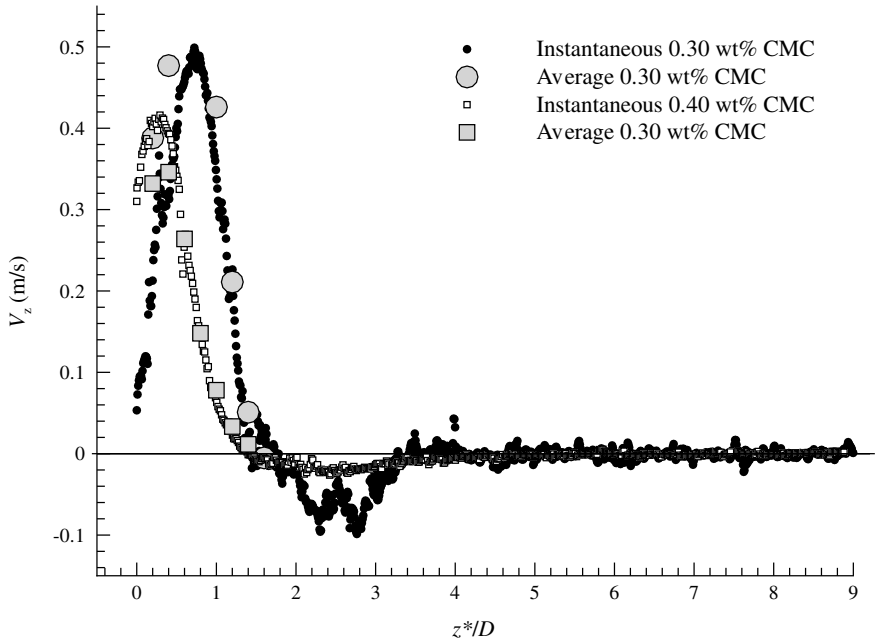

Fig. 10. Representation of the instantaneous and average vertical liquid velocity at the axis of the column as a function of the distance to the trailing edge of Taylor bubbles rising in 0.30 wt% and 0.40 wt% CMC solutions.

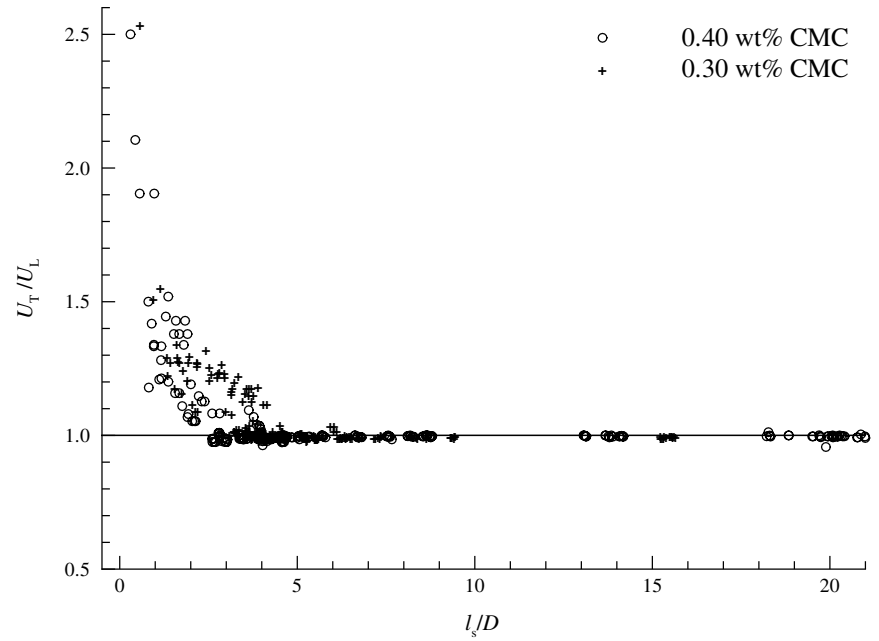

Fig. 11. Representation of the ratio between the velocities of trailing and leading bubbles as a function of the distance between bubbles for the 0.30 wt% and 0.40 wt% CMC solutions.

is a small portion of liquid rising up at the bubble velocity confirming the presence of a "positive" small wake. However, if in Fig. 14 we compare the 0.10 wt%, 0.30 wt% and 0.40 wt% CMC solutions with the predictions of the correlations found by Pinto and Campos (1996), Eqs. (1)–(3), it is possible to conclude that the low concentration CMC solutions behave in a manner very similar to that found in Newtonian solutions. For this

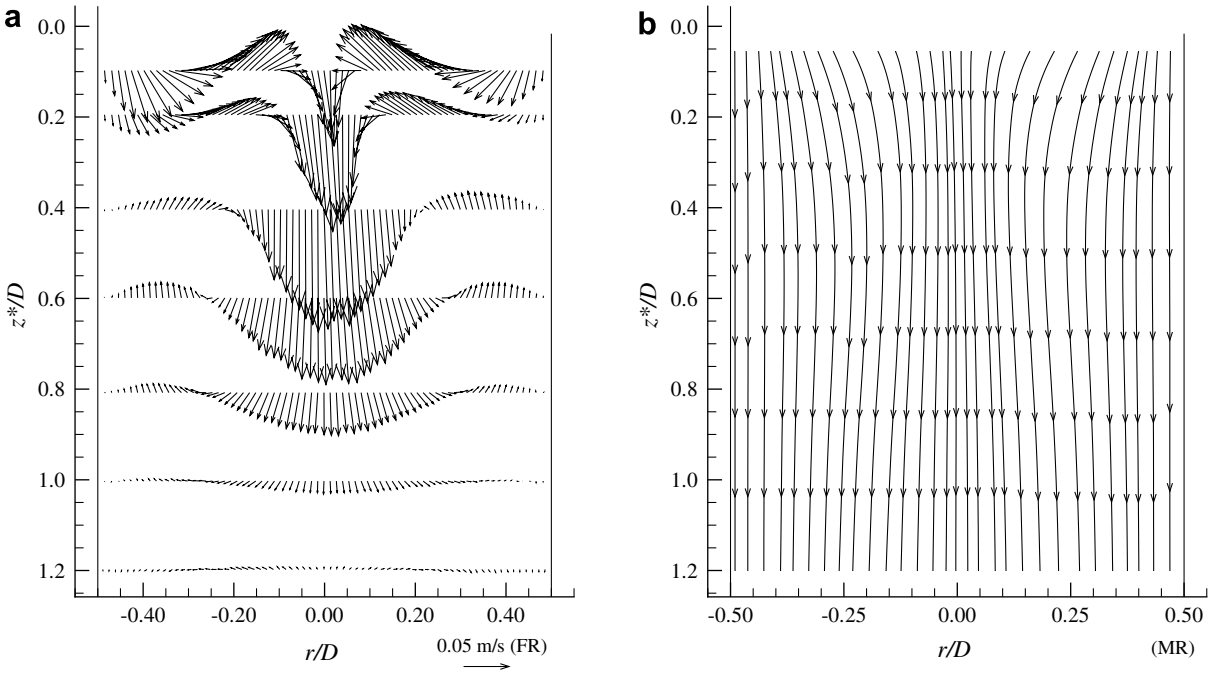

Fig. 12. (a) Average flow field (fixed reference frame) and (b) streamlines (reference frame moving with the bubble) in the wake of Taylor bubbles rising in a 0.80 wt% CMC solution.

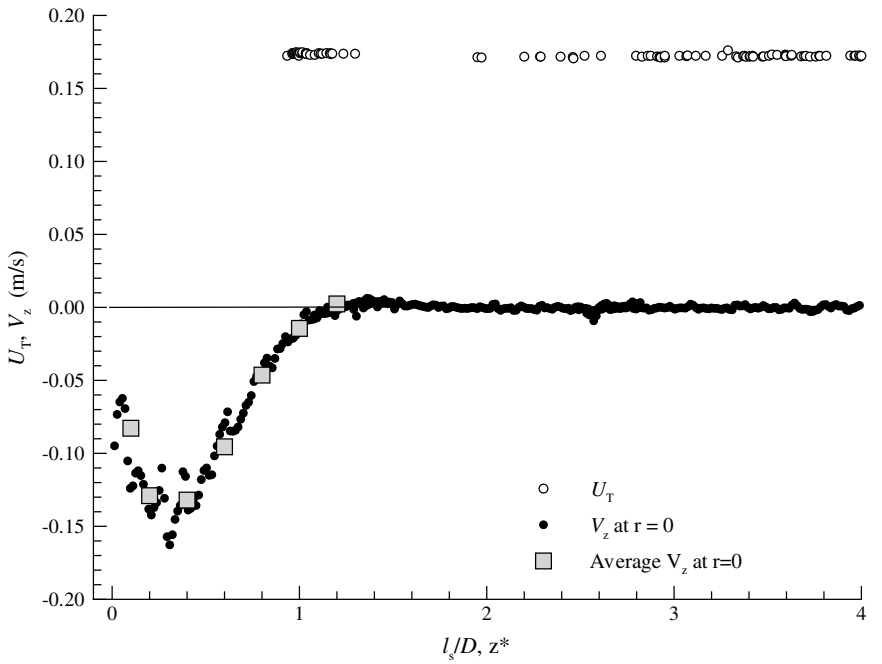

Fig. 13. Representation of the instantaneous and average vertical liquid velocity at the axis of the column as a function of distance to bubble trailing edge and the trailing bubble velocity as a function of the distance between bubbles, for a 0.80 wt% CMC solution.

comparison, the N_f number for non-Newtonian solutions was computed with the shear viscosity used to determine the Reynolds number (see Section 3).

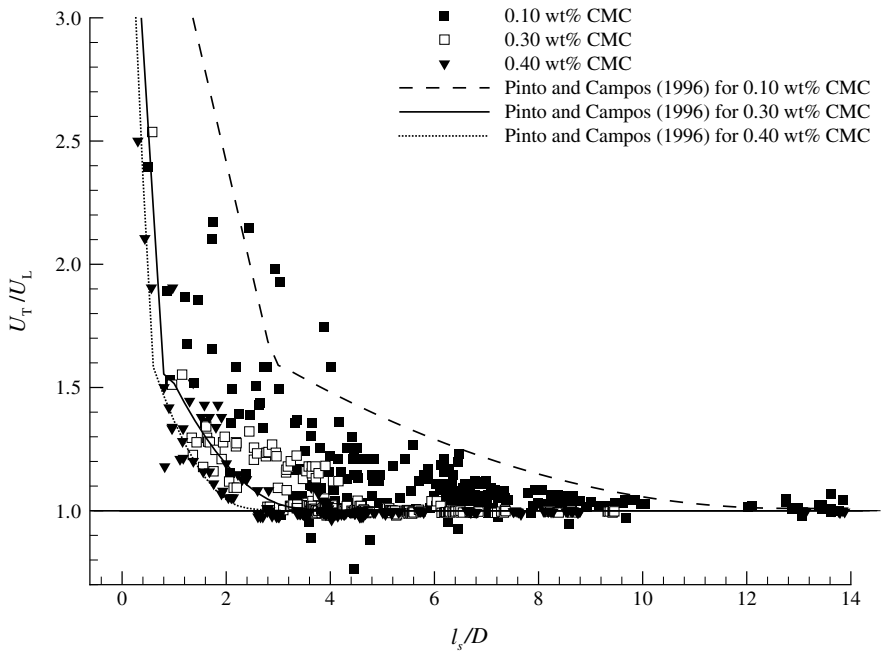

Fig. 14. Comparison of the ratio between the velocities of the trailing and leading bubbles for the 0.10 wt%, 0.30 wt% and 0.40 wt% CMC solutions with the correlations from Pinto and Campos (1996).

4.2. PAA solutions

The PAA solutions, despite having a moderate shear viscosity, show higher viscoelasticity than the CMC solutions. In the 0.10 wt% and 0.20 wt% PAA solutions, the flow fields obtained with the PIV technique showed that the wake flow pattern was different from those found in CMC solutions. The wake lengths were much longer and the liquid in the axis of the column was continuously being stretched while moving upwards for several column diameter lengths. These features can be seen by the average flow field in the wake of Taylor bubbles rising in a 0.10 wt% PAA solution, represented in Fig. 15 and the respective streamlines in a reference frame moving with the bubble, represented in Fig. 16. This far-reaching upward liquid movement is responsible for the acceleration of the trailing bubble at a greater distance from the leading one than for the CMC solutions. In Fig. 17, the trailing bubble velocity and the instantaneous and average vertical liquid velocity at the axis of the column are represented as a function of the distance to the leading bubble.

This figure clearly shows the relation between the increase in the vertical liquid velocity and the increase in the trailing bubble velocity as the distance to the leading bubble decreases. The trailing bubble velocity starts to increase faster below $l_s = 10D$, which is a much longer distance than those found in the CMC solutions. Besides the longer wake length in the PAA solutions, due to higher relaxation times the viscosity of the liquid when the trailing bubble is passing is lower than the viscosity of the liquid ahead of the leading bubble. This phenomenon is responsible for a less resistant path for the trailing bubble, which is clearly seen in Fig. 18 by plotting the ratio between the bubbles velocity as a function of the distance between them. Although for distances above $l_s = 10D$ the liquid is practically stagnant, the ratio between the bubble velocities is higher than 1 up to a distance of at least $60D$.

For the 0.20 wt% PAA solution the general behaviour is similar, although the acceleration of the trailing bubble occurs for lower distances from the leading bubble (around $l_s = 6D$), as shown in Fig. 19, due to a shorter wake length. The ratio between the bubble velocities remains higher than 1 now up to $90D$, as shown in Fig. 20. Bubble interaction was tested for distances up to $250D$, corresponding to around 40 s between bubble injections, and at this distance the trailing bubble still had a slightly higher velocity than the leading one. This is a much longer period than the relaxation time found in the rheological tests (see Table 2). This phe-

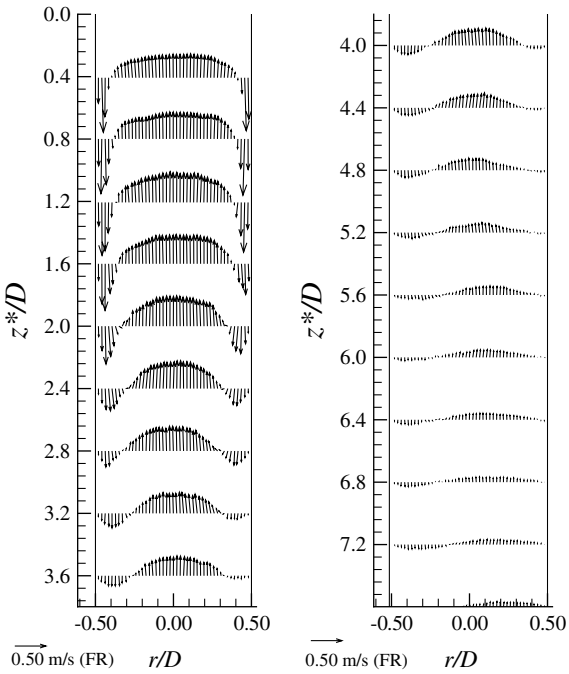

Fig. 15. Average flow field in the wake of Taylor bubbles rising in a 0.10 wt% PAA solution.

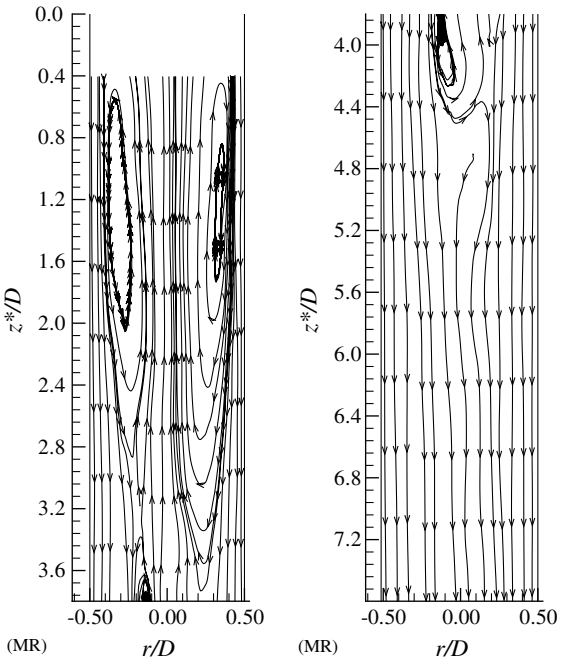

Fig. 16. Streamlines (reference frame moving with the bubble) in the wake of Taylor bubbles rising in a 0.10 wt% PAA solution.

nomenon was also observed in the sedimentation of spheres through viscoelastic fluids (Ambeskar and Mashelkar, 1990). In these experiments, long-lasting effects (from minutes to several hours) were observed for fluids with relaxation times on the order of several seconds. A number of explanations have been postulated, including stress-induced migration and the formation of a long-range structure or order in the fluid, but

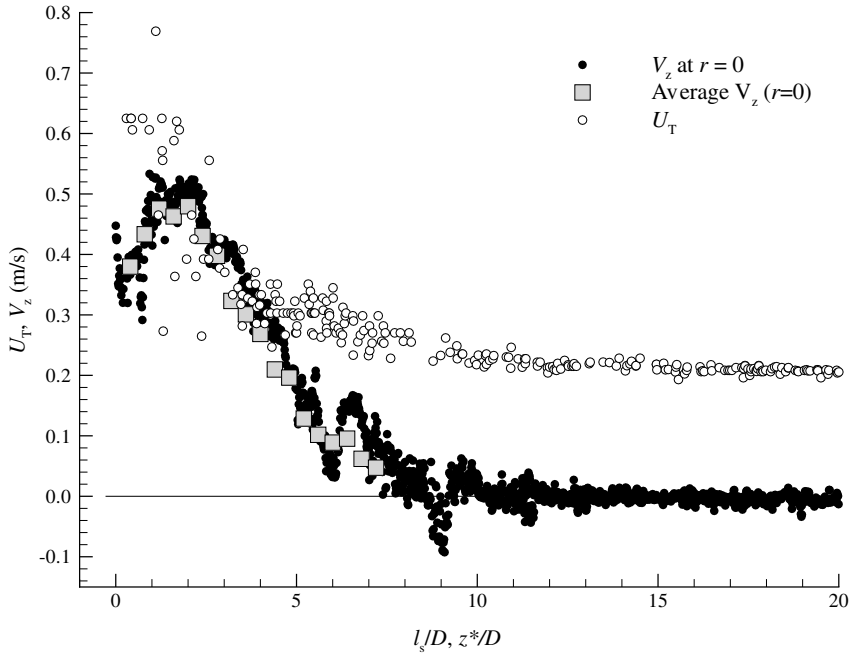

Fig. 17. Representation of the instantaneous and average vertical liquid velocity at the axis of the column as a function of the distance to the bubble trailing edge and of the trailing bubble velocity as a function of the distance between bubbles, for the 0.10 wt% PAA solution.

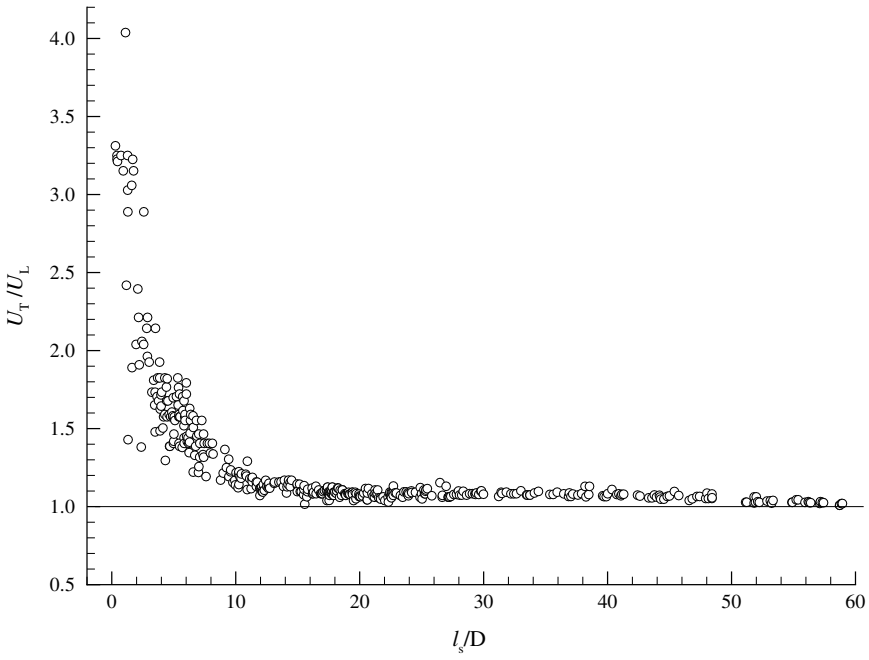

Fig. 18. Representation of the ratio between the trailing bubble velocity and the leading bubble velocity for the 0.10 wt% PAA solution.

this is a phenomenon that has yet to be fully explained or resolved. In more concentrated PAA solutions negative wakes were also observed (Sousa et al., 2006), but the long-lasting effects did not allow a more detailed study.

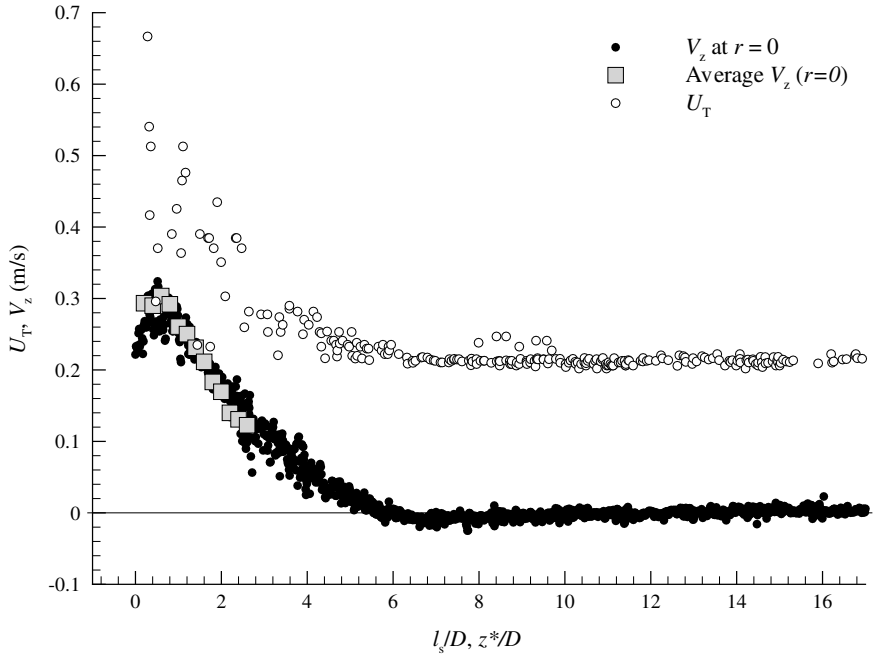

Fig. 19. Representation of the instantaneous and average vertical liquid velocity at the axis of the column as a function of the distance to bubble trailing edge and of the trailing bubble velocity as a function of the distance between bubbles, for the 0.20 wt% PAA solution.

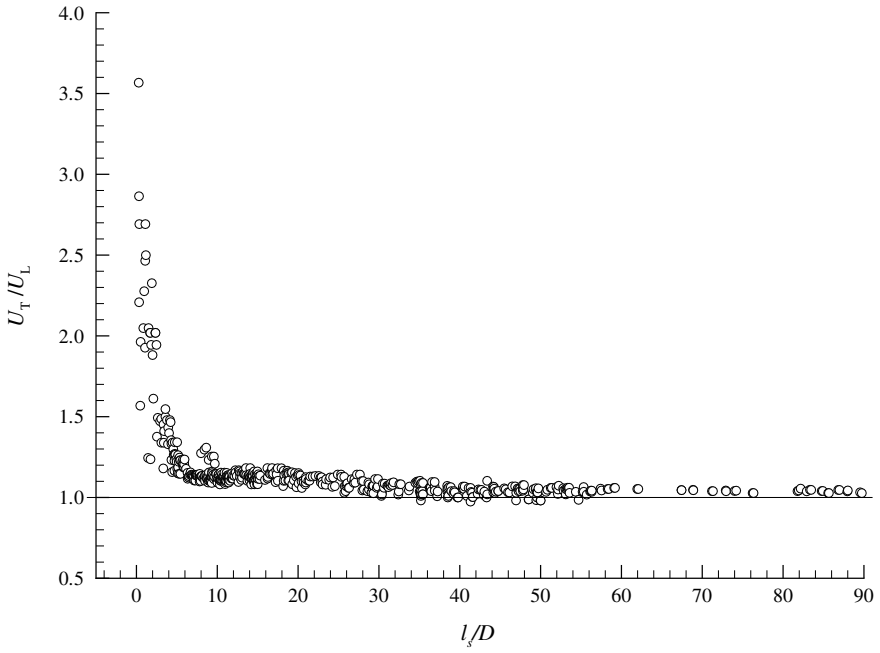

Fig. 20. Representation of the ratio between the trailing bubble velocity and the leading bubble velocity for the 0.20 wt% PAA solution.

5. Conclusions

This work presents experimental data on the interaction between consecutive Taylor bubbles rising in non-Newtonian solutions. For the least concentrated CMC solutions, with moderate shear viscosity and low

viscoelasticity the interaction was shown to be similar to that found in Newtonian fluids. For fluids with low relaxation times, the trailing bubble velocity is mainly dependent on the liquid velocity in the wake of the leading bubble. For the most viscous CMC solution, with high viscosity and moderate elasticity, a negative wake forms behind the Taylor bubbles, inhibiting coalescence since the bubbles maintain a minimum distance of about $1D$ between them during their rise. For the PAA solutions, with moderate shear viscosity and a viscoelasticity higher than the CMC solutions, the longer wake lengths are responsible for trailing bubble acceleration at greater distances from the leading bubble. Also, due to long relaxation times, the time needed for the fluid to recover its initial shear viscosity after the passage of the first bubble makes the fluid less resistant to the trailing bubble flow. Hence, the trailing bubble travels at a higher velocity than the leading bubble, even at distances above $90D$. This work presents new and relevant data, which contribute to the understanding of the interaction mechanism of Taylor bubbles in non-Newtonian fluids.

Acknowledgements

Financial support for this study was given by F.C.T., SFRH/BD/3389/2000, and von Karman Institute provided the experimental setup. This work was also supported, via CEFT, by POCTI (FEDER).

References

Ambeskar, V., Mashelkar, R.A., 1990. On the role of stress-induced migration on time-dependent terminal velocities of falling spheres. Rheol. Acta 29, 182–191.

Campos, J.B.L.M., Guedes de Carvalho, J.R.F., 1988. An experimental study of the wake of gas slugs rising in liquids. J. Fluid Mech. 196, 27–37.

Kee, D.D., Chhabra, R.P., Dajan, A., 1990. Motion and coalescence of gas bubbles in non-Newtonian polymer solutions. J. Non-Newton. Fluid Mech. 37, 1–18.

Leider, P.J., Bird, R., 1974. Squeezing flow between parallel disks. I. Theoretical analysis. Ind. Eng. Chem. Fundam. 13, 336.

Li, H.Z., Mouline, Y., Choplin, L., 1997a. Rheological simulation of in-line bubble interactions. AIChE J. 43, 265–267.

Li, H.Z., Mouline, Y., Choplin, L., Midoux, N., 1997b. Chaotic bubble coalescence in non-Newtonian fluids. Int. J. Multiphase Flow 23, 713–723.

Li, H.Z., Mouline, Y., Funfschilling, D., Marchal, P., Choplin, L., Midoux, N., 1998. Evidence for in-line bubble interactions in non-Newtonian fluids. Chem. Eng. Sci. 53, 2219–2230.

Li, H.Z., Frank, X., Funfschilling, D., Mouline, Y., 2001. Towards the understanding of bubble interactions and coalescence in non-Newtonian fluids: a cognitive approach. Chem. Eng. Sci. 56, 6419–6425.

Moissis, R., Griffith, P., 1962. Entrance effects in a two-phase slug flow. J. Heat Transfer Trans. ASME Ser. C 2, 29–39.

Nogueira, S., 2005. Hydrodynamic characterisation of gas–liquid slug flow: numerical and experimental investigation. Ph.D. thesis, Faculdade de Engenharia da Universidade do Porto.

Pinto, A.M.F.R., Campos, J.B.L.M., 1996. Coalescence of two gas slugs rising in a vertical column of liquid. Chem. Eng. Sci. 51, 45–54.

Pinto, A.M.F.R., Pinheiro, M.N.C., Campos, J.B.L.M., 1998. Coalescence of two gas slugs rising in a co-current flowing liquid in vertical tubes. Chem. Eng. Sci. 53, 2973–2983.

Pinto, A.M.F.R., Pinheiro, M.N.C., Campos, J.B.L., 2001a. On the interaction of Taylor bubbles rising in two-phase co-current slug flow in vertical columns: turbulent wakes. Exp. Fluids 31, 643–652.

Pinto, A.M.F.R., Pinheiro, M.N.C., Nogueira, S., Ferreira, V.D., Campos, J.B.L.M., 2005. Experimental study on the transition in the velocity of Taylor bubbles in vertical upward two-phase slug flow. Chem. Eng. Res. Des. 83, 1103–1110.

Shemer, L., Barnea, D., 1987. Visualization of the instantaneous velocity profiles in gas–liquid slug flow. Physico Chemical Hydrodynam. 8, 243–253.

Sousa, R.G., 2005. Flow of Taylor bubbles rising in stagnant non-Newtonian fluids. Ph.D. thesis, Faculdade de Engenharia da Universidade do Porto.

Sousa, R.G., Nogueira, S., Pinto, A.M.F.R., Riethmuller, M.L., Campos, J.B.L.M., 2004. Flow in the negative wake of a Taylor bubble rising in viscoelastic carboxymethylcellulose solutions: particle image velocimetry measurements. J. Fluid Mech. 511, 217–236.

Sousa, R.G., Riethmuller, M.L., Pinto, A.M.F.R., Campos, J.B.L.M., 2005. Flow around individual Taylor bubbles rising in CMC solutions: PIV measurements. Chem. Eng. Sci. 60, 1859–1873.

Sousa, R.G., Riethmuller, M.L., Pinto, A.M.F.R., Campos, J.B.L.M., 2006. Flow around individual Taylor bubbles rising in stagnant polyacrylamide (PAA) solutions. J. Non-Newton. Fluid Mech. 135, 16–31.

Talvy, C.A., Shemer, L., Barnea, D., 2000. On the interaction between two consecutive elongated bubbles in a vertical pipe. Int. J. Multiphase Flow 26, 1905–1923.